

Physics in non-fixed spatial dimensions

Ioannis Kleftogiannis

Physics Division, National Center for Theoretical Sciences, Hsinchu 30013, Taiwan

E-mail: ph04917@yahoo.com

Ilias Amanatidis

Department of Physics, Ben-Gurion University of the Negev, Beer-Sheva 84105, Israel

Abstract. We study the quantum statistical electronic properties of random networks which inherently lack a fixed spatial dimension. We use tools like the density of states (DOS) and the inverse participation ratio (IPR) to uncover various phenomena, such as unconventional properties of the energy spectrum and persistent localized states (PLS) at various energies, corresponding to quantum phases with zero-dimensional (0D) and one-dimensional (1D) order. For small ratio of edges over vertices in the network RT we find properties resembling graphene/honeycomb lattices, like a similar DOS containing a linear dispersion relation at the band center at energy $E=0$. In addition we find PLS at various energies including $E=-1,0,1$ and others, for example related to the golden ratio. At $E=0$ the PLS lie at disconnected vertices, due to partial bipartite symmetries of the random networks (0D order). At $E=-1,1$ the PLS lie mostly at pairs of vertices (bonds), while the rest of the PLS at other energies, like the ones related to the golden ratio, lie at lines of vertices of fixed length (1D order), at the spatial boundary of the network, resembling the edge states in confined graphene systems with zig-zag edges. As the ratio RT is increased the DOS of the network approaches the Wigner semi-circle, corresponding to random symmetric matrices (Hamiltonians) and the PLS are reduced and gradually disappear as the connectivity in the network increases. Finally we calculate the spatial dimension D of the network and its fluctuations, obtaining both integer and non-integer values and examine its relation to the electronic properties derived. Our results imply that universal physics can manifest in physical systems irrespectively of their spatial dimension. Relations to emergent spacetime in quantum and emergent gravity approaches are also discussed.

1. Introduction

The concept of spatial dimension has been central in physics for many centuries. Physics problems are usually formulated mathematically on geometrical manifolds with a well defined spatial dimension, which is taken as an input. However in the last decades problems like quantum and emergent gravity and geometry, have shown that a reconsideration of this concept is required. For example models like, string theory formulated on continuous manifolds (membranes) of variable dimensions higher than three [1, 2], or discrete/network/graph models like loop quantum gravity [3, 4], causal set cosmology [5, 6, 7, 8] the Wolfram-Gorard-Piskunov model [9, 10] and others [11, 12, 13, 14], hint that spatial dimension as a fundamental concept has to be revised, if spacetime and its dimensionality is to be recovered as emergent from other more fundamental structures. Also, problems like the small value of the cosmological constant, which could be an intrinsic property of spacetime as it emerges from other structures is a major related issue. All the above are strong suggestions that a theory reproducing the properties of spacetime in our universe, gravity and quantum effects could be spatio-dimensionless in its nature. Apart from quantum and emergent gravity, physics in non-fixed spatial dimensions can be useful in characterizing

quantum and other phases phenomena emerging in many-body systems[15, 16, 17], that could be also relevant to emergent spacetime and its dimensionality, through entanglement[15].

In this paper we consider spatio-dimensionless physical systems, modelled via the most structureless models, random networks[18, 19], which are discrete mathematical models that do not inherently have a fixed spatial dimension. We consider uniform networks and study their quantum statistical electronic properties, using tools like the density of states(DOS) and the inverse participatio ratio(IPR). We find that for small ratio of edges over vertices in the network RT its electronic properties resemble those of graphene/honeycomb lattices with properties like linear dispersion relation at the band center at energy $E=0$ and edge states concentrated at the spatial boundary of the network [20, 21, 22, 23, 24]. We find persistent localized states (PLS) at various energies including $E=-1,0,1$ and others, for example related to the golden ratio, via the study of the DOS and the IPR. These states comprise primarily of single unconnected vertices (0D order) at $E=0$ and one-dimensional(1D) clusters (1D order) for the other energies, where the wavefunction is localized. The energy of these 1D ordered states is determined by the dispersion of 1D tight-binding chains formed by the 1D clusters of various lengths. The 0D ordered states at $E=0$ spread over the whole network, while the 1D ordered states are concentrated at the spatial boundary of the network, resembling the edge states in confined graphene systems with zig-zag edges[20, 21, 24]. As the number of edges between the vertices in the network increases, the DOS approaches the Wigner semicircle, corresponding to ensembles or random symmetric matrices, and the number of PLS is gradually reduced until they disappear for large RT . Finally we calculate the spatial dimension D of the networks, i.e. the dimension of the manifold in which they can be embedded. We find that the networks which resemble graphene have $D \approx 2$, fitting into a 2D plane. The dimension is increased logarithmically as RT increases and the network becomes more dense as more edges are added between its vertices. Additionally D reaches integer values like $D \approx 4$ apart from non-integer ones. Our results show that universal phenomena can manifest in physical systems irrespectively of their spatial dimension. In addition we briefly discuss the relation of our results to emergent spacetime and relativity/gravity from discrete mathematical models.

2. Network model

Random networks are discrete mathematical models comprising of many vertices randomly connected with edges[18, 19]. They can be used to express relations between different quantities, which is useful for example in simulating various real world behaviors such as propagation of behavioral patterns in social networks or in communications technology. Random networks are also useful in studying various localization phenomena in mesoscopic and random waveguide systems, theoretically and experimentally[25]. The probability distribution of the number of edges at each vertex (degree deg) determines the type of network. In the current paper we choose the most simple type, uniform networks whose degree at each vertex follows a box distribution. Essentially we have a fixed number of vertices n and edges m between them randomly distributed forming a random network $G(n, m)$. All configurations of the edges among the vertices, whose number is $\binom{n}{m}$, have an equal probability to appear. The mean degree for each vertex in the uniform network is given by $\langle deg \rangle = 2\frac{m}{n}$ which can be interpreted as the average connectivity in the network. Note, there are no multi-edges or loops namely the network is a simple undirected graph. We define the ratio of vertices over the edges in the network $RT = \frac{m}{n}$, which is half its average connectivity $RT = \frac{\langle deg \rangle}{2}$.

We examine how a quantum particle behaves as it propagates through the tight-binding lattice formed by the random network. i.e. the electronic properties of the random network. The Hamiltonian of the system can be written as

$$H = \sum_{\langle i,j \rangle}^m (c_i^\dagger c_j + h.c.) \quad (1)$$

where $c_i^\dagger(c_i)$ is the creation(annihilation) operation for a particle at vertex i in the random network.

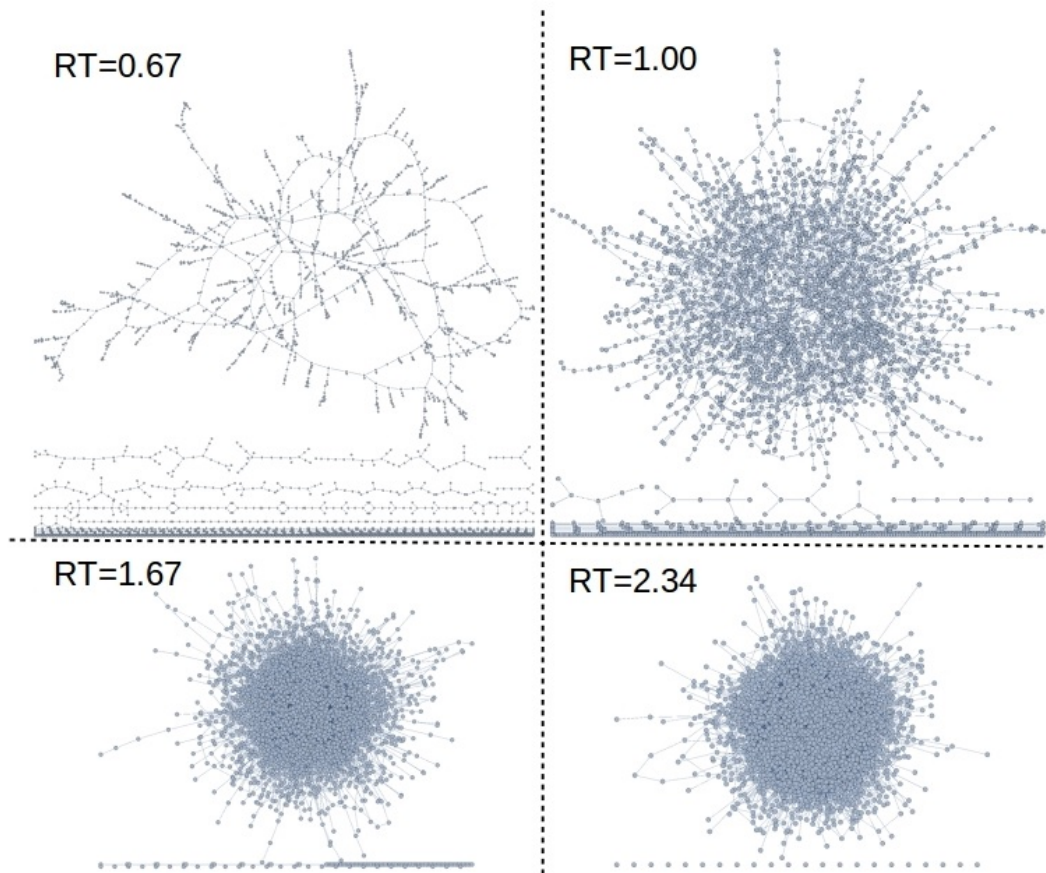


Figure 1. Various random networks for different values of the the ratio between the number of edges over the number of vertices RT . The number of vertices is $n=3000$ for all the cases shown. For $RT = 0.67$ the network is almost planar with few overlapping edges, meaning that it can be fitted approximately into a 2D plane. As more edges are added RT increases and the network becomes spatially more dense.

The indexes i,j are randomly sampled and create m pairs, representing the edges between the vertices in the network. The Eq. 1 is a random matrix with a fixed number of elements m (the number of edges) with the value of one, randomly distributed inside the matrix. In certain cases, such random network Hamiltonians have been shown to belong to the same universality class as models used to study Anderson localization phenomena[25]. For example regular tight-binding lattices like the square or the cubic lattice with a random on-site potential (Anderson model). The randomly distributed elements in the Hamiltonian matrix Eq. 1 induce interference effects leading to localization of the wavefunctions as in the Anderson model or in random matrix theory(RMT) models.

3. Energy spectrum

In this section we examine the properties of the energy spectrum of the random networks via the distribution of eigenvalues of Eq. 1, i.e. the density of states (DOS) of the random network. Firstly there are two limiting cases worth mentioning. When all the n vertices in the network are disconnected ($m=0$) then all the elements of the Hamiltonian Eq. 1 are zero resulting in n zero eigenvalues and a DOS localized at energy $E=0$. On the other hand when all the vertices in the network are connected

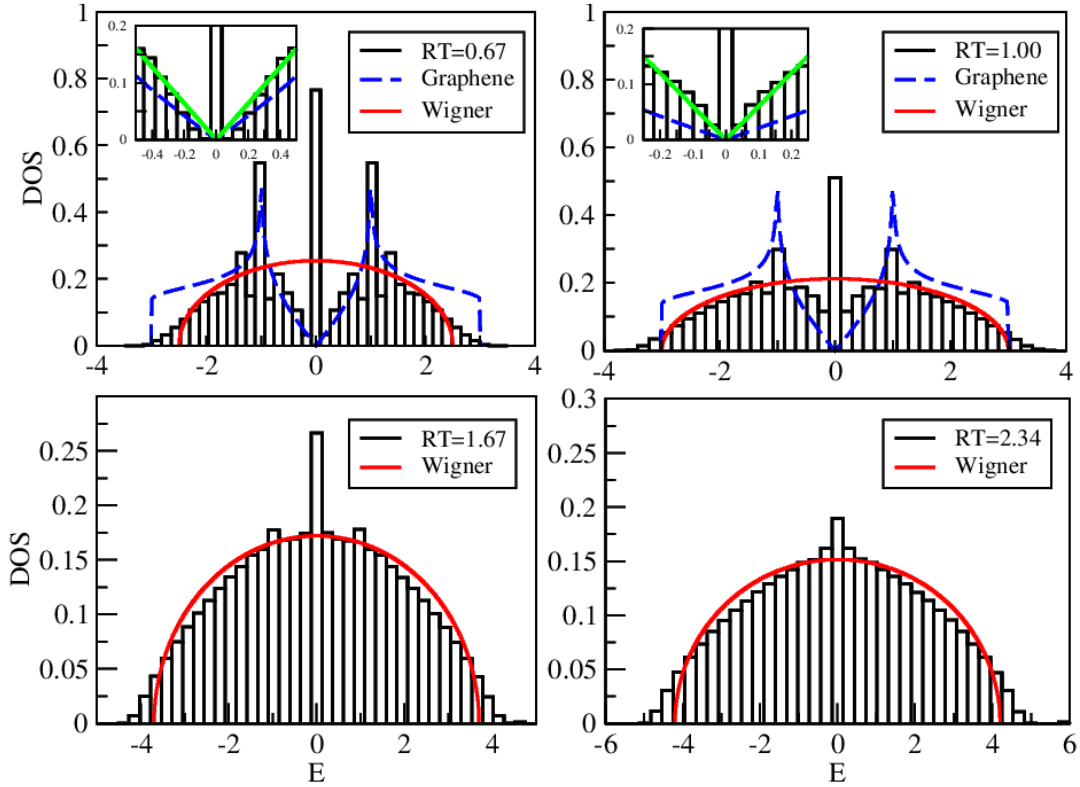


Figure 2. The distribution of eigenvalues for the networks, i.e. the density of states (DOS) for various values of the ratio of edges over vertices RT , represented by the black boxes. We have considered 100 different configurations/realizations of the network (runs). The DOS in the upper panels contain features from graphene/honeycomb lattice systems, as shown from the comparison with the graphene DOS represented by the blue dashed curve. A linear behavior of the DOS is shown in the insets as for graphene. As RT increases and the network becomes more dense the DOS starts resembling the distribution of eigenvalues of random symmetric matrices, the Wigner semi-circle represented by the red curves. A prominent peak at $E=0$ is present in all cases coming from many states at this energy persistent for all networks.

with each other, the Hamiltonian is full apart from its diagonal which has all its elements equal to zero. In the intermediate case, for an arbitrary number of vertices n and edges m in the network we have found two major forms for the DOS. The results are shown in Fig. 2. In the plots we have removed the eigenvalues $E=0$ coming from disconnected vertices in the network which lead to lines/columns of zeros in the Hamiltonian. For low ratio RT in the two upper panels of Fig. 2 the DOS of the random network resembles that of a graphene/honeycomb lattice as can be seen from the comparison between the blue dotted line and the histogram. The main features are two peaks at energies $E=-1,1$ appearing in both cases and a linear dispersion $DOS(E) = \alpha|E|$ near $E=0$ shown in the insets of the upper panels. We note that for low RT there is a large probability that the network contains many disconnected components as shown in Fig. 1. We have found that these components largely contribute in the number of states appearing at $E=-1,1$. Another main feature is a peak at $E=0$ which appears also for confined graphene systems with zig-zag edges like flakes and nanoribbons, due to edge states at $E=0$ [20, 21, 24]. We examine the localization properties of these states in the following sections. The resemblance to graphene can be seen schematically by the network presented in the upper left panel of

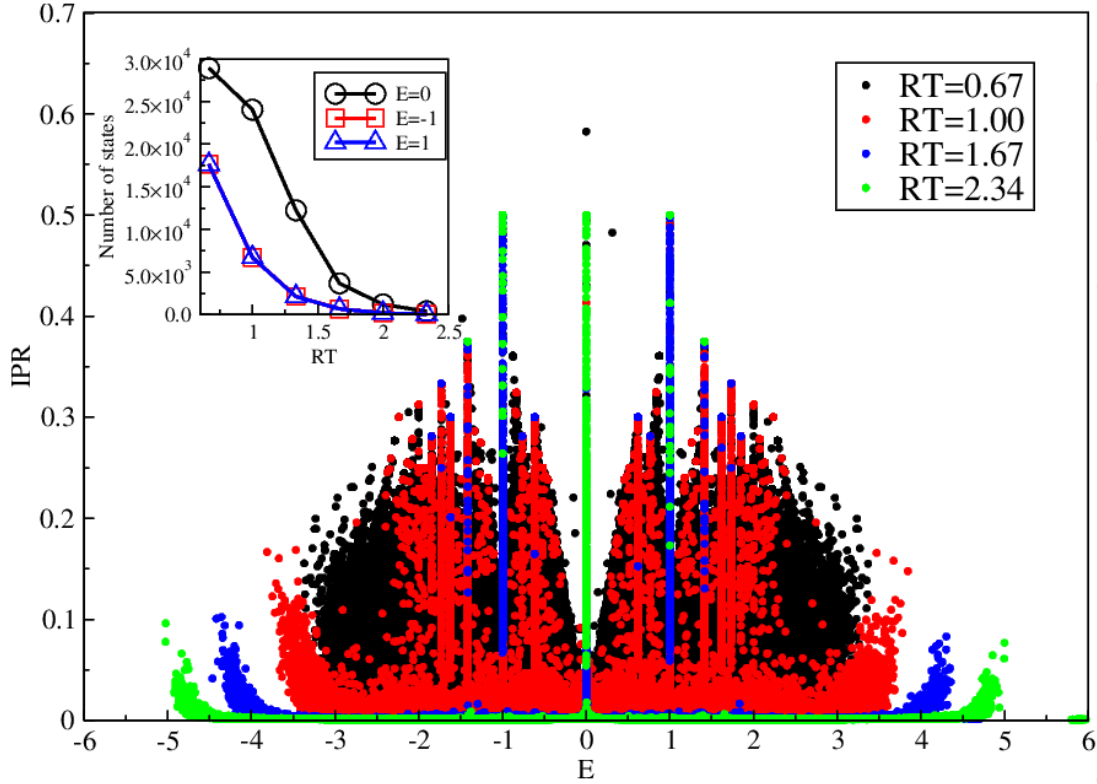


Figure 3. The inverse participation ratio (IPR) for various values of the ratio of the number of edges over the number of vertices in the network, for 100 runs. The states across the whole energy spectrum become in average less localized as the network becomes more dense, with increasing RT . Various persistent localized states (PLS) can be distinguished at various energies including $E=-1,0,1$ where IPR forms vertical lines with high values. The number of PLS at $E=-1,1$ is gradually decreased with increasing RT .

Fig. 1. The network consists primarily of triangles and polygons whose corners consist of vertices that are connected mostly to three or four neighboring vertices. In addition there are rarely any crossing edges, i.e. the network is approximately planar, meaning that it can be fitted into a two-dimensional(2D) plane. This structure is very similar to a graphene/honeycomb lattice which is a 2D plane of hexagons with every lattice site having three neighboring sites, i.e. the connectivity is three.

The peaks at $E=-1,0,1$ and the linear dispersion near $E=0$, gradually disappear as RT increases as can be seen in the lower panels of Fig. 2. As more edges are added in the network its Hamiltonian starts to resemble ensembles of random symmetric matrices whose distribution of eigenvalues follow the Wigner semicircle, as the size of the matrices approach infinity. The Wigner semicircle function is defined as

$$f(x) = \begin{cases} \frac{2}{\pi R^2} \sqrt{R^2 - x^2} & -R \leq x \leq R \\ 0 & otherwise \end{cases} \quad (2)$$

The above equation for various R is represented by the red continuous curve in Fig. 2 and describes sufficiently the DOS for the cases shown in the lower panels. Some features of the DOS at its edges are also captured by the Wigner semicircle in the upper panels for low RT . In overall we see that the DOS of the random network contains features from both graphene/honeycomb lattices and disordered systems described by random symmetric matrices(Hamiltonians). The contribution of these two systems on the electronic properties of the network depends on the value of RT , which determines the spatial density

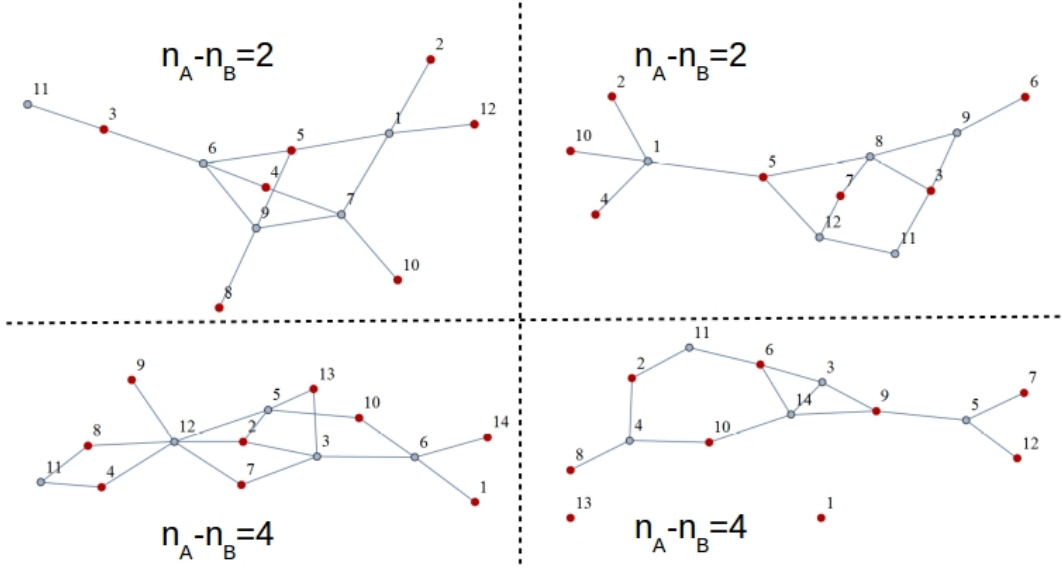


Figure 4. Some examples of small networks demonstrating the partial bipartite symmetry. Red vertices form a sublattice of disconnected vertices (A) while the rest of the vertices form another sublattice (B). The difference in the number of vertices/sites between the two sublattices $n_A - n_B$ leads to an equal number of $E=0$ states. The wavefunction of these states is zero on the B sublattice which has the least number of sites.

of the network. Sparse networks for low RT resemble graphene, while dense networks for large RT resemble disordered systems.

The main difference with regular lattices such as the square, the cubic and the hypercubic is that their DOS reaches gradually a Gaussian distribution as the lattice connectivity, i.e. the number of neighbors at each site in the lattice goes to infinity.

4. Localization properties

In Fig. 3 we show the inverse participation ratio (IPR) for the wavefunctions of Eq. 1 defined as

$$IPR(E) = \sum_{i=1}^n |\Psi_i(E)|^4 \quad (3)$$

where i runs over the all the vertices and Ψ is the corresponding wavefunction amplitude. We show IPR for 100 different configurations/realizations of the network (runs). There are two major features that we can observe. As RT increases and the network becomes spatially more dense, IPR decreases in average. This means that the corresponding wavefunctions become in average less localized with increasing RT . We have verified that these wavefunctions corresponding to low values of IPR spread over the whole network with random amplitudes at each vertex, resembling chaotic wavefunctions encountered in disordered tight-binding lattices[26, 27]. Another major feature that we can observe in Fig. 3 is persistent localized states (PLS) appearing at various energies corresponding to high values of IPR , forming persistent vertical lines for all RT . We can clearly distinguish PLS at energies $E=-1,0,1$ which correspond to peaks in the DOS shown in Fig. 2. As shown in the inset of Fig. 3 the number of these states are reduced as RT increases. We have found that the states at $E=0$ are localized at vertices along the whole network which are not connected by edges. All the $E=0$ states are localized on the same vertices albeit with different amplitudes. This is one main feature of the $E=0$ states for all RT and differs

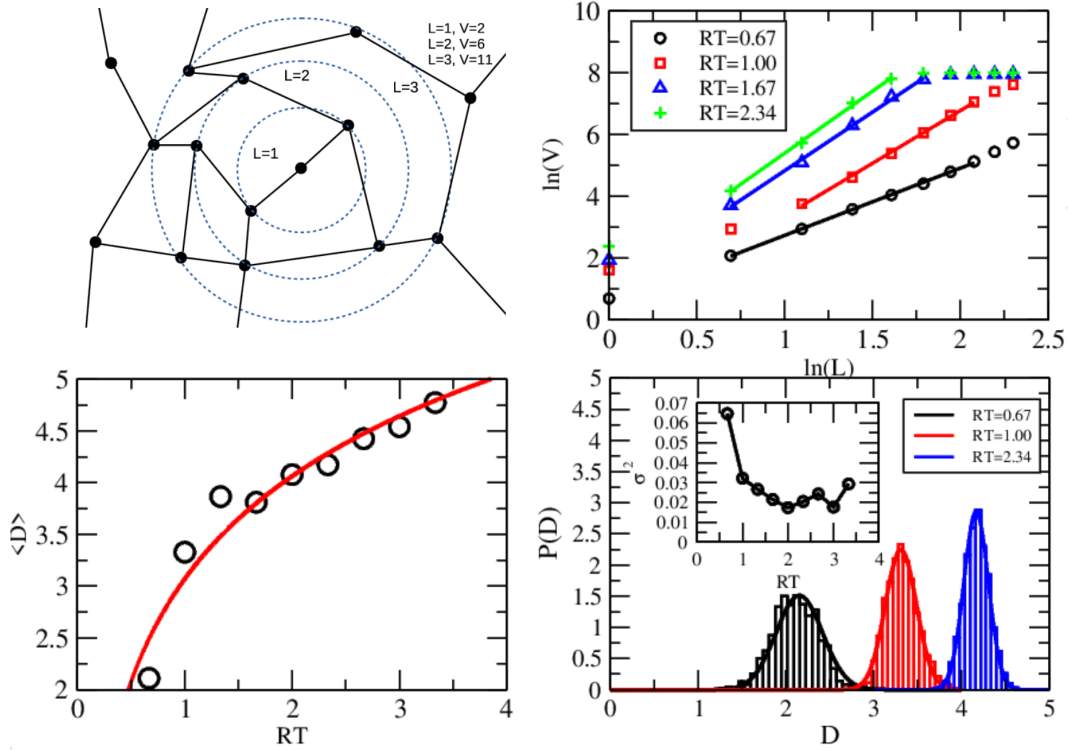


Figure 5. Upper left panel: The process of calculating the spatial dimension D of the network by counting how the number of vertices contained into a spherical volume of radius L grows with L . The number of vertices added at each step by increasing L are determined by the edges/connections between the vertices. Upper right panel: The linear scaling of $\ln(V)$ with $\ln(L)$ gives the value of the dimension D from the relation $V \approx L^D$. Lower left panel: The mean value of D (open circles) for 1000 configurations/realizations (runs) of the network versus the ratio RT . Integer and non-integer values like $D \approx 4$ are reached. The dimension follows a logarithmic behavior $D \approx \log(RT = \frac{\langle \text{deg} \rangle}{2})$ represented by the fitting red curve, as for regular lattices of integer dimension like the square and the cube. Lower right panel: The propability distribution of D follows the normal (Gaussian) distribution whose variance is decreased with increasing RT as shown in the inset.

from confined graphene systems with zig-zag edges which contain edge states at $E=0$ concentrated at the boundary of the system [20, 21, 24]. We can consider that the PLS at $E=0$ in the network, form a quantum phase of zero-dimensional (0D) order, since the wavefunction lies only on disconnected vertices. On the other hand we have found that the PLS at $E=-1,1$ are concentrated only at the spatial boundary of the network and localize mostly on pairs of vertices connected with an edge (bonds). This bond-ordered localized phase disappears for large RT indicating a phase transition at some critical value of RT . On the other hand the $E=0$ states persist even for large RT as shown by the peaks in the DOS in Fig. 2. Other cases of PLS appear also at other energies for example at $E = -\phi, -1 + \phi, 1 - \phi, \phi$ where $\phi = \frac{(1+\sqrt{5})}{2}$ is the so called golden ratio. The wavefunctions of these states are localized primarily on lines of vertices (1D clusters) with fixed length, for example lines of four vertices for the energies related to the golden ratio, instead of bonds, and disappear for large RT as for the PLS at $E=-1,1$. All the phases except those at $E=0$ can be considered as quantum phases of one-dimensional (1D) order. We have found that the energies of these 1D ordered states are coming from tight-binding chains whose length is determined by the length of the 1D clusters contained in the 1D ordered phases. The dispersion of a tight-binding chain

with N sites is given by

$$E = 2 \cos \frac{n\pi}{N+1}, n = 1, 2, \dots, N. \quad (4)$$

The networks contain mostly the eigenvalues of the above equation for low N corresponding to short chains. For example some of the $E=-1,1$ eigenvalues in the network come from Eq. 4 for $N=2$ (chain with two sites) and the corresponding wavefunctions are localized along bonds of vertices. The case $N=4$ gives the energies related to the golden ration. In general, the wavefunctions of the states in the network coming from Eq. 4 are localized along lines of vertices of length N and lie at the spatial boundary of the network, connected with one edge to the rest of the vertices, resembling dangling bonds. In this sense these 1D ordered states at energies coming from Eq. 4 bear similarity to the edge states appearing in confined graphene systems, like flakes and ribbons, which are concentrated along the zig-zag edges of these systems[20, 21, 24] and persist even with disorder[27]. Also, a large contribution to the eigenvalues Eq. 4 comes from disconnected chains in the network of length N .

5. Partial bipartite symmetry

The appearance of the $E=0$ wavefunctions only on vertices of the network that are not directly connected with an edge can be explained as a consequence of a partial bipartite symmetry of the random networks[28, 29, 30]. The random network if seen as a lattice can always be split into two sublattices, say A and B with n_A and n_B sublattice sites respectively. Additionally it can always be splitted in such a way that there are no edges between the sites in one of the sublattices, say A. Then the Hamiltonian of the system can be simplified if written in the basis of A and B sites, as

$$H = \begin{bmatrix} 0 & H_{AB} \\ H_{AB}^\dagger & H_{BB} \end{bmatrix}. \quad (5)$$

We can write the Schrodinger difference equations centered on A and B sites as

$$\begin{aligned} E\Psi_{A,i}^\mu &= \sum_j \Psi_{B,j} \\ E\Psi_{B,i}^\mu &= \sum_j \Psi_{A,j} + \sum_k \Psi_{B,k} \end{aligned} \quad (6)$$

By setting $E=0$ we can see that the upper equation in Eq. 6 transforms to $\sum_j \Psi_{B,j} = 0$ which is a set of n_A equations with n_B unknowns. If $n_A > n_B$ then this set of equations can only be satisfied by setting $\Psi_{B,j} = 0$ since there are more equations than unknowns i.e. the system of equations is overdetermined. Then the amplitudes on A sublattice $\Psi_{A,k}$ can be calculated by the lower equation in Eq. 6, which is a system of n_B equations with n_A unknowns and gives $n_A - n_B$ linearly independent solutions. Consequently if the random network is split in two sublattices A and B, with one of them having no edges between its vertices, say A, whose number of vertices is larger than the number of vertices for the other sublattice B, then there will always exist at least $n_A - n_B$ states at $E=0$. In addition the wavefunction of these states will have zero amplitudes on the sublattice with the smallest number of vertices, sublattice B. We remark that for periodic lattices like the square lattice which satisfy the full bipartite symmetry the value $n_A - n_B$ will depend on the shape of the boundary. For example for a square sample of square lattice we will always have $n_A - n_B = 1$ [28] whereas in graphene flakes $n_A - n_B$ depends on the size of the system[30]. Depending on the network configuration(run) there exist in general many different choices of the sublattice whose vertices are disconnected, corresponding to different partial bipartite symmetries. Note that in rare cases and more frequently in small networks with a low number of vertices and edges, some of equations for the sublattice A might be identical reducing the total number of equations for A. If the number of these equations becomes smaller than the number of B sites then the argument presented above breaks down and the wavefunctions spreads on both sublattices for the $E=0$ states. Nevertheless the partial bipartite symmetry is present for any type of random network and will lead to $E=0$ states with the properties described above in most cases of networks with low spatial density corresponding to low ratio of edges over vertices RT .

6. Spatial dimension

In this section we examine the spatial dimension of the random networks, i.e. the dimension of the ambient space in which they can be embedded. This can be achieved by examining how the connected vertices fill an ambient space of dimension D , which can take integer or non-integer values. One example of this process can be seen schematically in the upper left panel of Fig. 5. At each step in the scaling characterized by the linear length scale L we count the number of vertices that are connected directly with edges to the previous layer with $L-1$. This number is added in the overall volume V , which counts the total number of vertices contained in a spherical volume of radius L . Therefore by calculating the growth of V with L we can calculate the dimension D of the network via

$$V \sim L^D. \quad (7)$$

Some results of this process for different RT can be seen in the upper right panel of Fig. 5. In addition in the lower left panel we plot the average $\langle D \rangle$ for 1000 runs (configurations/realizations of the random network). For $RT = 0.67$ the network is almost planar as $D \approx 2$, fitting into a 2D plane. This is one of the reasons that the sparse networks resemble graphene/honeycomb lattices and have similar electronic properties, as we have shown in the previous sections by the comparison between the DOS of the two systems. As the network becomes spatially more dense due to the increased connectivity, D grows logarithmically with RT represented by the fitting red curve in the lower left panel of Fig. 5. Integer and non-integer dimensions like $D \approx 2$ and $D \approx 4$ are reached. However the electronic properties of the networks, as we have shown in the previous sections, do not resemble the respective regular lattices of integer dimension D , like hypercubic lattices, whose DOS approaches a Gaussian distribution as D increases. Instead the DOS of the random networks follows the Wigner semicircle, resembling disordered systems described by random symmetric Hamiltonians. A logarithmic dependence of the spatial dimension on the connectivity can be derived for regular lattices like the square and the cubic. The connectivity deg at each site in these lattices is four(eight) for the square(cube), giving in general a logarithmic form $deg = 2^D \Rightarrow D \sim \log(deg)$. Our result in the lower left panel of Fig. 5 shows that this behavior is valid even for non-integer dimensions. Since $RT = \frac{\langle deg \rangle}{2}$ the dimension of the random network depends exponentially on its average connectivity at each vertex $\langle deg \rangle$, as for the regular lattices, despite the non-integer dimensions reached by the random networks. In the lower right panel of Fig. 5 the probability distribution of D is shown along with the variance σ^2 (fluctuations) in the inset. All the distributions are normal (Gaussian). The fluctuations are reduced as RT increases, corresponding to higher dimension and spatially denser networks.

7. Emergent spacetime and relativity/gravity

In this section we discuss briefly the relation of our model with the notion of emergent spacetime and relevant relativistic and gravitational effects. A natural way, in the sense of being the most structureless lacking an inherent spatial dimension, would be to consider spacetime or space as a collection of random relations between abstract objects, sometimes called atoms of space[3, 4, 5, 6, 7, 8, 9, 10, 12, 13, 14], with various constraints. These relations can be naturally modeled by random networks, with the abstract objects(relations) represented by the vertices(edges), and the constraint in our case being the fixed ratio defined as the number of edges over the number of vertices RT . Essentially space could be represented as a quantum mechanical superposition of the different realizations of the random networks for fixed RT . Then one of the main issues would be if the network can be reduced to a continuous manifold at a limit of large number of vertices and whether geometry can emerge in such a system. For instance, when $RT = 0.67$ in the random network that we studied, its spatial dimension is $D \approx 2$ resembling a 2D plane. Moreover its electronic properties, as indicated by the DOS, resemble those of graphene, which is a 2D honeycomb lattice with the electrons following the Dirac equation near low energies $E=0$. Electrons in graphene behave relativistically as massless particles with the speed of light c being replaced by the Fermi velocity of the electrons v_f , with linear energy dispersion $E = v_f k$. The similarities of

the electronic properties between graphene and spatially sparse random networks, pose an intriguing question, whether relativistic effects are also encountered in those random networks. We remark also that $D \approx 4$ is reached at $RT=2$, when the number of edges is double the number of vertices, which would be tempting to relate to 4D spacetime in the models describing our universe. We note that time in network/graph models can be integrated either in the network itself[6, 7, 8] or can be treated as an external updating rule[9, 10].

In addition gravitational effects could potentially emerge in a random network approach to space. Various definitions of the curvature at each vertex in the network exist[31, 32, 33, 34, 35], the simplest one being for tree and grid graphs

$$K(i) = 1 - \frac{\text{deg}(i)}{2}. \quad (8)$$

where $\text{deg}(i)$ is the number of connected neighbors at vertex i in the network. Moreover the Ricci curvature tensor can be calculated in graph/network models[31, 33]. In addition geodesics can be defined in the network as simply the path between two vertices that has the least number of edges. Again an intriguing question arises, whether the curvature in the network can be related to the Riemannian curvature used in Einstein's field equations to describe how the geometry of spacetime, influenced by the mass-energy distribution, gives rise to gravitational effects. The density of vertices in the network could represent mass while edges can be related to the energy[9, 10]. In this sense the PLS that we have found in the networks at various energies, comprising of lines of vertices (1D order), could be loosely interpreted as emergent particles, whose mass is determined by the number of vertices in these 1D structures.

The general question of how geometry arises from discrete mathematical models is fundamental issue in both mathematics and physics. Another related problem is how to construct mathematics and physical theories in non-integer spatial dimensions or in the complete absence of spatial dimensions like the approach that we follow in the current manuscript, using random networks.

8. Summary and Conclusions

We have studied the quantum statistical electronic properties of random networks which inherently lack a fixed spatial dimension. We have found that the electronic properties of network contain features from graphene/honeycomb lattice systems and disordered systems described by random symmetric Hamiltonians. The similarities to graphene occur for spatially sparse networks with low ratio of edges over vertices RT and include features like linear energy dispersion relation at the band center at $E=0$ and various persistent localized states (PLS) concentrating at the spatial boundary of the networks, resembling the edge states in graphene systems with zig-zag edges. The PLS occur at various energies for example at $E=-1,0,1$ and others related for example to the golden ratio, and are localized either at single unconnected vertices (0D order) or lines of vertices of fixed length which determines their energy (1D order). As the network becomes spatially more dense its electronic properties, indicated for example by the DOS start to resemble disordered systems described by random symmetric Hamiltonians whose distribution of eigenvalues follows the Wigner semi-circle. The PLS apart from those at $E=0$ gradually disappear as RT increases and the network becomes more dense, with more edges between its vertices. Finally we have calculated the dimension D of the ambient space in which the networks can be embedded. We have found a logarithmic growth of D with RT , reaching integer and non-integer values, implying an exponential dependence of the average connectivity in the network to D as in regular lattices which have integer D . In summary we have studied quantum mechanics in physical systems lacking a fixed spatial dimension, demonstrating various unconventional electronic properties. These properties could be universal for quantum mechanical systems irrespectively of their spatial dimension. Finally we have discussed the relation of our results to spacetime and relativistic/gravity effects that could emerge from discrete mathematical models, like the random networks that we considered.

Acknowledgements

We acknowledge resources and financial support provided by the National Center for Theoretical Sciences of R.O.C. Taiwan and the Department of Physics of Ben-Gurion University of the Negev in Israel. Also we acknowledge support by the Project HPC-EUROPA3, funded by the EC Research Innovation Action under the H2020 Programme. In particular, we gratefully acknowledge the computer resources and technical support provided by ARIS-GRNET and the hospitality of the Department of Physics at the University of Ioannina in Greece.

References

- [1] Mukhi S 2011 *Class. Quantum Grav.* **28** 153001
- [2] Dienes K R 1997 *Phys. Rept.* **287** 447 [hep-th/9602045]
- [3] Rovelli C 2011 *Class. Quantum Grav.* **28** 153002
- [4] Rovelli C 2008 *Living Rev. Relativ.* **11** 5
- [5] Bombelli L, Lee J, Meyer D and Sorkin R D 1987 *Phys. Rev. Lett.* **59** 521-524.
- [6] Dowker F 2014 *Annals of the New York Academy of Sciences* **1326**, 18725
- [7] Dowker F and Zalel S 2017 *C R Physique* **18**:246-253.
- [8] Surya S 2019 *Living Rev. Rel.* **22** 5 (2019), arXiv:1903.11544 [gr-qc]
- [9] Wolfram S 2020 *Complex Systems* **29**(2) pp. 107-1536.
- [10] Gorard J 2020 *Complex Systems*, **29**(2) pp. 599-654.
- [11] Laughlin R B 2003 *Int. J. Mod. Phys. A* **18**, 831
- [12] Lombard J 2017 *Phys. Rev. D* **95** 024001
- [13] Verlinde E J 2011 *High Energ. Phys.* **29**
- [14] Trugenberger, C.A., *J. High Energ. Phys.* 2017, 45
- [15] Christandl M, Datta N, Ekert A and Landahl A 2004 *Phys. Rev. Lett.* **92**, 187902
- [16] Walschaers M, Fernandez-de-Cossio Diaz J, Mulet R and Buchleitner A 2013 *Phys. Rev. Lett.* **111**, 180601
- [17] Ortega A, Stegmann T and Benet L 2016 *Phys. Rev. E* **94**, 042102
- [18] Newman M E J *Networks: An Introduction* (Oxford University Press, Oxford, 2010)
- [19] Frieze A, Karonski M: *Introduction to random graphs.* Cambridge University Press (2015)
- [20] Nakada K, Fujita M, Dresselhaus G and Dresselhaus M S 1996 *Phys. Rev. B* **54** 17954
- [21] Wakabayashi K, Fujita M, Ajiki H and Sigrist M 1999 *Phys. Rev. B* **59** 8271
- [22] Novoselov K S et al. 2004 *Science* **306** 666
- [23] Geim A K and Novoselov K S 2007 *Nature Materials* **6** 183-191
- [24] Heiskanen H P et al 2008 *New J. Phys.* **10** 103015
- [25] Zhang Z-Q and Sheng P 1994 *Phys. Rev. B* **49** 83
- [26] Amanatidis I and Evangelou S N 2009 *Phys. Rev. B* **79** 205420
- [27] Klefogiannis I and Amanatidis I 2014 *Eur. Phys. J. B* **87** 16
- [28] Inui M, Trugman S A and Abrahams E 1994 *Phys. Rev. B* **49**, 3190
- [29] Klefogiannis I and Evangelou S N 2013 arXiv:1304.5968 [cond-mat.dis-nn]
- [30] Klefogiannis I and Amanatidis I 2016 *J. Phys.: Condens. Matter* **28** 045305
- [31] Forman R 2003 *Discrete Comput. Geom.* **29** 323
- [32] Hoorn P, Cunningham W J, Lippner G, Trugenberger C and Krioukov D 2020 *Phys. Rev. Research* **3** 013211
- [33] Ollivier Y 2013 In *Analysis and Geometry of Metric Measure Spaces.* CRM Proc. Lecture Notes 56 197-220. Amer. Math. Soc., Providence, RI. MR3060504
- [34] Samal A et al. 2018 *Sci. Rep.* **8**, 8650.
- [35] Knill O 2012 *Elemente der Mathematik* **67**,1, pp1-44 arXiv 1009.2292 2010; Knill O 2011 arXiv 1111.5395